

# $\Lambda_c - N$ interaction from lattice QCD

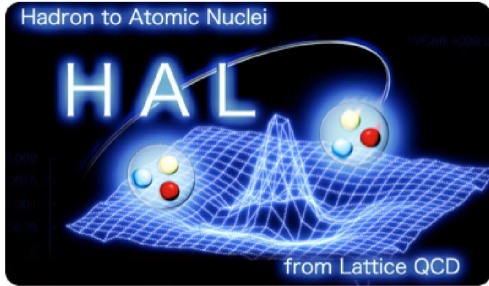
**Takaya Miyamoto\***

*Yukawa Institute for Theoretical Physics, Kyoto University*

*Sakyo-ku, Kyoto 606-8502 Japan*

*E-mail: takaya.miyamoto@yukawa.kyoto-u.ac.jp*

**for HAL QCD Collaboration**



We investigate the s-wave  $\Lambda_c - N$  interaction for spin singlet systems( $^1S_0$ ) using the HAL QCD method. In our lattice QCD simulations, we employ gauge configurations generated by the PACS-CS Collaboration at  $a = 0.0907(13)$  fm on a  $32^3 \times 64$  lattice ( $La = 2.902(42)$  fm). We employ two ensembles, one at  $m_\pi = 700(1)$  MeV and the other at  $m_\pi = 570(1)$  MeV to study the quark mass dependence of the  $\Lambda_c - N$  interactions. We calculate a  $^1S_0$  central potential not only for the  $\Lambda_c - N$  system but also for  $\Lambda - N$  system to understand the role of heavy charm quarks in  $\Lambda_c - N$  system. We find repulsion at short distance and attraction at mid-range for both the  $\Lambda_c - N$  and the  $\Lambda - N$  potentials. The short range repulsion of the  $\Lambda_c - N$  potential is smaller than that of the  $\Lambda - N$  potential, and the attraction of the  $\Lambda_c - N$  potential is small compared with the  $\Lambda - N$  potential. The phase shift and scattering length calculated with these potentials show that there exist no bound state for both the  $\Lambda_c - N$  and  $\Lambda - N$  systems for  $m_\pi > 570$  MeV.

*The 33rd International Symposium on Lattice Field Theory*

*14 -18 July 2015*

*Kobe International Conference Center, Kobe, Japan*

\*Speaker.

## 1. Introduction

The heavy hadron physics attracts our attention, since there are many exotic hadrons such as  $X(3872)$  discovered by Belle experiment [1], which do not fit into the quark model interpretation. They are considered to be composite states of two (or more) hadrons including heavy quark(s). If attractions between hadrons are same, heavier hadrons are easier to form a bound state due to their smaller kinetic energy. Therefore, it is important to investigate the interaction of heavy hadron.

Almost 40 years ago,  $\Lambda_c$ -nucleus bound states, charmed nuclei, were predicted [2], where  $\Lambda_c(2286)$  was considered as the lightest charmed baryon. It was, however, inconclusive whether the 2-body system of  $\Lambda_c - N$  has a bound state or not. Recently, a possibility of such a bound state has been pointed out based on the meson-exchange model [3, 4], though no bound state has been observed for its counterpart of hyperon,  $\Lambda - N$ . In the heavy quark region, the channel coupling has important effects for  $\Lambda_c - N$  bound state because the mass threshold of  $\Sigma_c N$  and  $\Sigma_c^* N$  to be close due to the heavy quark spin symmetry and  $\Sigma_c^* N$  bring strong attractive tensor force coming from one-pion exchange.

The results of model calculation are rather sensitive to details of interactions at the short distance. Therefore the investigations based on QCD are mandatory for a definite conclusion on the existence of the  $\Lambda_c - N$  bound state. Recently, an approach to investigate hadron interactions in lattice QCD has been proposed by the HAL QCD Collaboration [5, 6, 7] and extensively developed [8, 9, 10, 11, 12, 13, 14]. Since the HAL QCD method can be easily extended to charmed-baryons interactions, we have investigated the  $\Lambda_c - N$  interaction using this method, as the first step to understand charmed-baryon interactions in lattice QCD.

In this paper, we present our results of  $\Lambda_c - N$  interactions in the  $^1S_0$  state at two gauge configurations corresponding to  $m_\pi = 700(1)$  MeV and  $m_\pi = 570(1)$  MeV. For a comparison, we also give results on  $\Lambda - N$  ( $^1S_0$ ) system. Using these results, we extracted the phase shift and scattering length of both systems, and give our conclusion on the existence of the  $\Lambda_c - N$  bound state.

## 2. HAL QCD method

A key quantity in the HAL QCD method is the equal-time Nambu-Bethe-Salpeter (NBS) wave function, which encodes informations of scattering phase shifts in its asymptotic behavior [5, 6, 7]. The NBS wave function in the center-of-mass frame is defined by

$$\psi_{\alpha\beta}^{(W)}(\vec{r})e^{-Wt} = \sum_{\vec{x}} \langle 0 | B_{\alpha}^{(1)}(\vec{r} + \vec{x}, t) B_{\beta}^{(2)}(\vec{x}, t) | B^{(1)}(\vec{k}) B^{(2)}(-\vec{k}), W \rangle, \quad (2.1)$$

where  $|B^{(1)}(\vec{k}) B^{(2)}(-\vec{k}), W\rangle$  is the QCD eigenstate for two baryons system with mass  $m_{B^{(1)}}$  and  $m_{B^{(2)}}$ , relative momentum  $\vec{k}$ , total energy  $W = \sqrt{|\vec{k}|^2 + m_{B^{(1)}}^2} + \sqrt{|\vec{k}|^2 + m_{B^{(2)}}^2}$ , and  $B_{\alpha}(\vec{x}, t)$  is the local interpolating operator for baryon. In this work, we choose the following baryon operators for nucleon and  $\Lambda_c$ .

$$N_{\alpha}(x) \equiv \begin{pmatrix} p_{\alpha}(x) \\ n_{\alpha}(x) \end{pmatrix} = \varepsilon_{ijk} [u_i^T(x) C \gamma_5 d_j(x)] q_{k,\alpha}(x), \quad q(x) = \begin{pmatrix} u(x) \\ d(x) \end{pmatrix}, \quad (2.2)$$

$$\Lambda_{c\alpha}(x) = \varepsilon_{ijk} [u_i^T(x) C \gamma_5 d_j(x)] c_{k,\alpha}(x), \quad (2.3)$$

where  $x = (\vec{x}, t)$ ,  $i, j, k$  are the color indices, while  $\alpha$  is the spinor index,  $C$  is the charge conjugation matrix defined by  $C = \gamma_2 \gamma_4$ ,  $p(x), n(x)$  are the proton and neutron operators, and  $u(x), d(x), c(x)$  denote up-, down- and charm-quark operators, respectively.

From the NBS wave function, we define the non-local potential through the following Schrödinger-type equation,

$$(E_n - H_0) \psi^{(W_n)}(\vec{r}) = \int d^3 r' U(\vec{r}, \vec{r}') \psi^{(W_n)}(\vec{r}'), \quad \left( E_n = \frac{k_n^2}{2\mu}, H_0 = \frac{-\nabla^2}{2\mu} \right), \quad (2.4)$$

where  $\mu$  is the reduced mass of the two baryon system. At low energy, it is useful to introduce the derivative expansion of the non-local potential,

$$U(\vec{r}, \vec{r}') = V(\vec{r}, \vec{\nabla}) \delta^{(3)}(\vec{r} - \vec{r}'). \quad (2.5)$$

where the local potential  $V(\vec{r}, \vec{\nabla})$  is given by

$$V(\vec{r}, \vec{\nabla}) = V_0(\vec{r}) + V_\sigma(\vec{r})(\vec{\sigma}_1 \cdot \vec{\sigma}_2) + V_T(\vec{r})S_{12} + \mathcal{O}(\vec{\nabla}), \quad (2.6)$$

$$S_{12} = 3 \frac{(\vec{r} \cdot \vec{\sigma}_1)(\vec{r} \cdot \vec{\sigma}_2)}{|\vec{r}|^2} - (\vec{\sigma}_1 \cdot \vec{\sigma}_2). \quad (2.7)$$

where  $\vec{\sigma}_i$  is the Pauli matrix acting on the spin index of the  $i$ -th baryon. For the s-wave spin-singlet state  $\psi_{1S_0}^{(W_n)}$ , we can extract the central potential as

$$V_C(\vec{r}) \equiv V_0(\vec{r}) - 3V_\sigma(\vec{r}) = \frac{(E_n - H_0) \psi_{1S_0}^{(W_n)}(\vec{r})}{\psi_{1S_0}^{(W_n)}(\vec{r})}. \quad (2.8)$$

The NBS wave function can be extracted from the baryon four-points correlation function on the lattice defined by

$$G_{\alpha\beta}(\vec{r}, t - t_0) = \sum_{\vec{x}} \langle 0 | B_\alpha^{(1)}(\vec{r} + \vec{x}, t) B_\beta^{(2)}(\vec{x}, t) \overline{\mathcal{J}^{(1,2)}}(t_0) | 0 \rangle. \quad (2.9)$$

where  $\overline{\mathcal{J}^{(1,2)}}(t_0)$  is the source operator which creates two baryon states. Inserting a complete set between the two-baryon operator and the source operator, we obtain

$$G_{\alpha\beta}(\vec{r}, t - t_0) = \sum_n \psi_{\alpha\beta}^{(W_n)}(\vec{r}) e^{-W_n(t-t_0)} A_n \quad (2.10)$$

$$\xrightarrow{(t-t_0) \rightarrow \infty} \psi_{\alpha\beta}^{(W_0)}(\vec{r}) e^{-W_0(t-t_0)} A_0, \quad (2.11)$$

with constant  $A_n = \langle B^{(1)}(\vec{k}) B^{(2)}(-\vec{k}), W_n | \overline{\mathcal{J}^{(1,2)}}(0) | 0 \rangle$ . In practice, we employ the time-dependent HAL QCD method [8] which does not require the grand state saturation for the extraction of potentials. In the non-relativistic approximation, the potential is extracted as

$$V(\vec{r}) = \frac{1}{R(\vec{r}, t - t_0)} \left[ \frac{1}{2(m_{B(1)} + m_{B(2)})} \frac{\partial^2}{\partial t^2} - \frac{\partial}{\partial t} - H_0 \right] R(\vec{r}, t - t_0), \quad (2.12)$$

where

$$R(\vec{r}, t - t_0) \equiv \frac{G(\vec{r}, t - t_0)}{e^{-m_{B(1)}(t-t_0)} e^{-m_{B(2)}(t-t_0)}}. \quad (2.13)$$

Note that if  $m_{B(1)} = m_{B(2)}$ , above equation is exact relativistic.

Hadron	Ensemble 1 ( $\kappa_{ud} = 0.13700$ , $\kappa_s = 0.13640$ )	Ensemble 2 ( $\kappa_{ud} = 0.13727$ , $\kappa_s = 0.13640$ )
$\pi$	700 (1) MeV	570 (1) MeV
$\phi$	1216 (3) MeV	1158 (6) MeV
$J/\psi$	3165 (1) MeV	3144 (1) MeV
$N$	1582 (7) MeV	1395 (4) MeV
$\Lambda$	1639 (6) MeV	1494 (5) MeV
$\Lambda_c$	2710 (5) MeV	2584 (4) MeV

**Table 1:** The hadron mass calculated on PACS-CS configurations. We use  $\kappa_c = 0.12240$  as hopping parameter for charm quark at both ensembles.

### 3. Numerical results

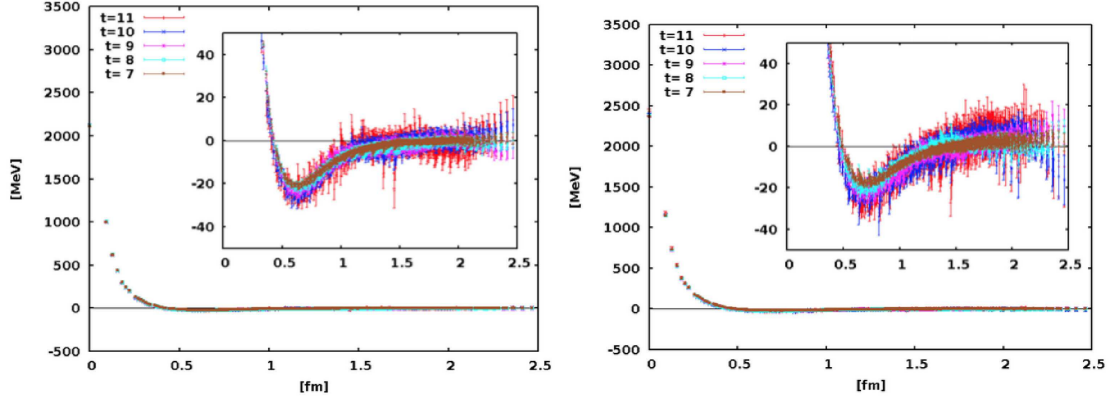
#### 3.1 Lattice setup

For numerical simulations, we have employed the  $2 + 1$  flavor full QCD configurations generated by PACS-CS Collaboration [15] with the renormalization-group improved Iwasaki gluon action and a nonperturbatively  $\mathcal{O}(a)$  improved Wilson-clover quark action. The lattice size is  $32^3 \times 64$  and the lattice spacing is  $a = 0.0907(13)$  fm (physical lattice size is  $La = 2.902(42)$  fm). In order to see the quark mass dependence of the potential, we have employed two ensembles of gauge configurations. The first ensemble generated at  $\kappa_{ud} = 0.13700$ ,  $\kappa_s = 0.13640$  corresponds to  $m_\pi = 700(1)$  MeV,  $m_\phi = 1216(3)$  MeV. The second ensemble generated at  $\kappa_{ud} = 0.13727$ ,  $\kappa_s = 0.13640$  corresponds to  $m_\pi = 570(1)$  MeV,  $m_\phi = 1158(6)$  MeV. We have calculated charm quark propagators at  $\kappa_c = 0.12240$  in (partial) quenched QCD. The hopping parameter of charm quark was determined in Ref.[16], so as to reproduce the mass of  $J/\psi$  (3097). Each hadron mass calculated on these configurations is given in Table 1. For statistics, we use 399 configurations  $\times$  4 sources for ensemble 1 and 400 configurations  $\times$  4 sources for ensemble 2.

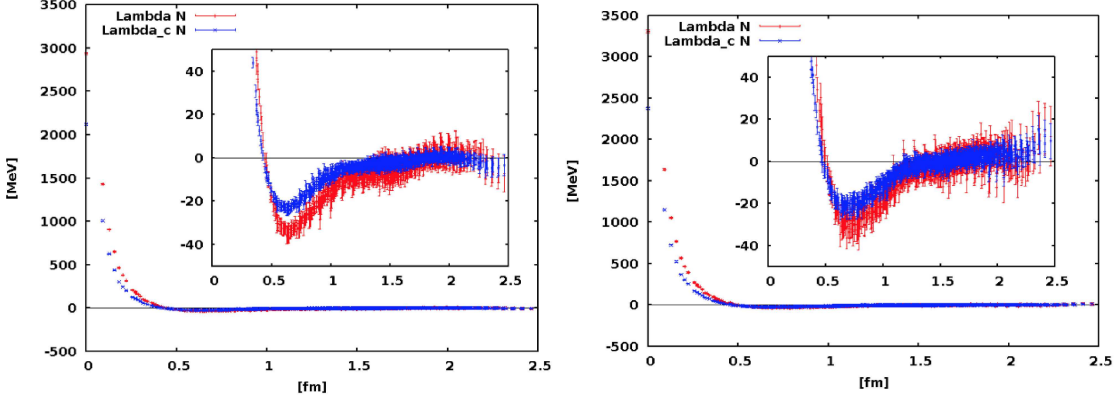
#### 3.2 Potentials

Fig.1 shows the time dependence of  $^1S_0$  central potential for  $\Lambda_c - N$  system. The left figure represents the potential on the ensemble 1 at  $m_\pi = 700(1)$  MeV, while the right one is the potential on the ensemble 2 at  $m_\pi = 570(1)$  MeV. Each figure shows the potential obtained at  $t - t_0 = 7, 8, 9, 10, 11$ . In both plots, the central potential has the repulsive core at short distance and the attractive pocket at medium distance. Fig.1 shows that potentials  $t - t_0 \geq 9$  are stable against the change of  $t - t_0$ . We therefore take  $t - t_0 = 9$  in the following analysis.

For a comparison, we also calculate the  $\Lambda - N$  potential on the same ensembles. Fig.2 shows the  $^1S_0$  central potential for both  $\Lambda - N$  and  $\Lambda_c - N$  systems in  $^1S_0$  channel at  $t - t_0 = 9$ . We observe that both repulsive core and attractive pocket of the  $\Lambda_c - N$  potential is weaker than those of the  $\Lambda - N$  potential. The behavior of smaller repulsive core in the  $\Lambda_c - N$  channel would be naturally explained by color magnetic interactions when the heavy quark spin symmetry for charm quarks is applied [4, 17]. Also we find the repulsive core becomes stronger as the quark mass decreases, while the attractive pocket does not show the strong quark mass dependence.



**Figure 1:** The  $^1S_0$  central potential for  $\Lambda_c - N$  system on the ensemble 1 at  $m_\pi = 700(1)$  MeV (Left) and on the ensemble 2 at  $m_\pi = 570(1)$  MeV (Right). Different colors represent different source-sink separations.



**Figure 2:** The  $^1S_0$  central potential for the  $\Lambda - N$  (Red) and the  $\Lambda_c - N$  (Blue) systems at  $t - t_0 = 9$ . The left figure represents the potential on the ensemble 1 at  $m_\pi = 700(1)$  MeV, while the right one show that on the ensemble 2 at  $m_\pi = 570(1)$  MeV.

### 3.3 Phase shift and scattering length

Once we obtain the potential, we can calculate the phase shift in the infinite volume. For this purpose, we fit the potential with the three-ranges gaussian functions given by

$$V(r) = a_1 e^{-\left(\frac{r}{b_1}\right)^2} + a_2 e^{-\left(\frac{r}{b_2}\right)^2} + a_3 e^{-\left(\frac{r}{b_3}\right)^2}. \quad (3.1)$$

Fitting parameters are given in Table 2 for both  $\Lambda - N$  and the  $\Lambda_c - N$  potentials on two ensembles. With the above result, we solved the Schrödinger equation by the difference method and the extracted the phase shift from the asymptotic form of wave function as

$$\psi_{k,l}(r) = A_l h_l^{(-)}(kr) + B_l h_l^{(+)}(kr), \quad (3.2)$$

where  $h_l^{(-)}(kr)$  and  $h_l^{(+)}(kr)$  are Hankel functions for the angular momentum  $l$ , and extracted the

Parameter	Ensemble 1		Ensemble 2	
	$\Lambda - N$ potential	$\Lambda_c - N$ potential	$\Lambda - N$ potential	$\Lambda_c - N$ potential
$a_1$	752 (23) MeV	514 (17) MeV	763 (31) MeV	525 (18) MeV
$b_1$	0.2567 (63) fm	0.2493 (70) fm	0.2904 (98) fm	0.2850 (93) fm
$a_2$	2210 (26) MeV	1629 (21) MeV	2540 (30) MeV	1861 (20) MeV
$b_2$	0.0947 (10) fm	0.0938 (10) fm	0.0997 (14) fm	0.0984 (12) fm
$a_3$	-55 (7) MeV	-41 (7) MeV	-70 (14) MeV	-55 (11) MeV
$b_3$	0.892 (70) fm	0.807 (70) fm	0.794 (75) fm	0.746 (63) fm

**Table 2:** The fitting results of the  $^1S_0$  central potential for the  $\Lambda - N$  and the  $\Lambda_c - N$  systems at the two ensembles. We use the three-ranges gaussian function Eq.(3.1) for the fitting function.

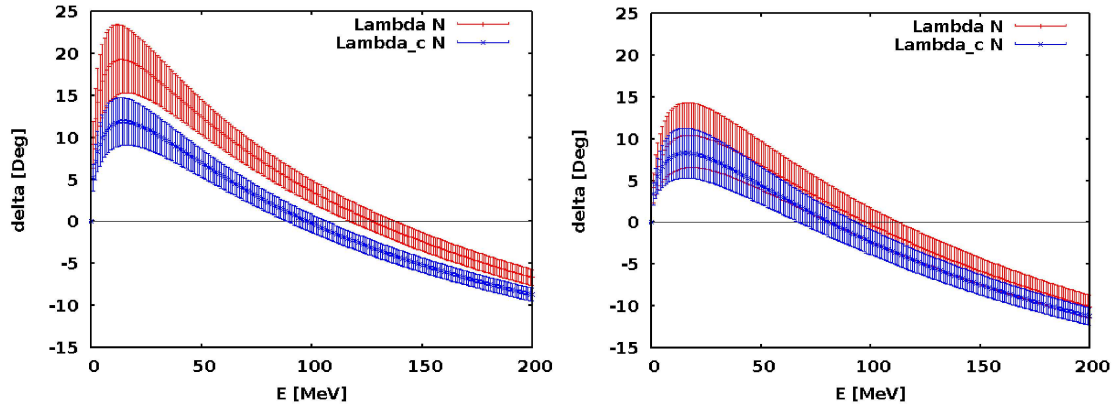


**Figure 3:** The phase shift for the  $\Lambda - N$  (Red) and the  $\Lambda_c - N$  (Blue) systems in  $^1S_0$  channel. The left figure represents the phase shift on ensemble 1 at  $m_\pi = 700(1)$  MeV, while the right one show that on ensemble 2 at  $m_\pi = 570(1)$  MeV.

ensemble	$\Lambda - N$	$\Lambda_c - N$
1	0.83 (27) fm	0.42 (13) fm
2	0.39 (17) fm	0.29 (11) fm

**Table 3:** The scattering length calculate by low energy limit of phase shift Eq.(3.3).

phase shift from the relation that  $S_l = e^{2i\delta_l} = \frac{B_l}{A_l}$ . Then the scattering length can be calculated as

$$a = \lim_{k \rightarrow 0} \frac{\tan \delta(k)}{k}. \quad (3.3)$$

Fig.3 shows the phase shift of the  $\Lambda - N$  and the  $\Lambda_c - N$  systems on two ensembles, while the scattering lengths are given in Table 3. From Fig.3 and Table 3, we see that there are no bound state for both  $\Lambda - N$  and  $\Lambda_c - N$  systems at both pion masses. Furthermore, we also observe that the net attraction of the  $\Lambda_c - N$  interaction is weaker than that of the  $\Lambda - N$  interaction at both pion masses, while the attractions of both systems become weaker as the pion mass decreases.

## 4. Summary

We have investigated the  $\Lambda_c - N$  interaction at  $^1S_0$  channel using the HAL QCD method. For a comparison, we have calculated the potential for  $\Lambda - N$  system as well, and have found that both repulsive core and attractive pocket of the  $\Lambda_c - N$  potential are weaker than those of the  $\Lambda - N$ 's. The behavior of the short range repulsion is naturally explained from color-spin interactions in quark models. From the potentials, we have extracted the phase shift and scattering length in the infinite volume for both systems, which show that both  $\Lambda_c - N$  and  $\Lambda - N$  systems do not form the two-body bound state at least  $m_\pi = 570$  and  $700$  MeV.

In our future work, we will calculate the potential for the  $\Lambda_c - N$  system in the  $J^P = 1^+$  channel, to investigate the effects of tensor force. Furthermore, we will study coupled-channel effects for the  $\Lambda_c N - \Sigma_c N - \Sigma_c^* N$  systems using the coupled-channel HAL QCD method [7, 14].

## Acknowledgments

We thank the PACS-CS Collaboration for providing us their  $2+1$  flavor gauge configurations [15]. Numerical computations of this work have been carried out by the KEK supercomputer system (BG/Q), [Project number : 14/15-21].

## References

- [1] S.-K. Choi et al. (Belle Collaboration), Phys. Rev. Lett. **91** (2003) 262001 [arXiv:hep-ex/0309032].
- [2] C. B. Dover and S. H. Kahana, Phys. Rev. Lett. **39** (1977) 1506.
- [3] Y. R. Liu, M. Oka, Phys. Rev. **D85** (2012) 014015 [arXiv:1103.4624 [hep-ph]].
- [4] S. Maeda, M. Oka, A. Yokota, E. Hiyama, Y. R. Liu [arXiv:1509.02445 [nucl-th]].
- [5] N. Ishii, S. Aoki and T. Hatsuda, Phys. Rev. Lett. **99** (2007) 022001 [nucl-th/0611096].
- [6] S. Aoki, T. Hatsuda and N. Ishii, Prog. Theor. Phys. **23** (2010) 89 [arXiv:0909.5585 [hep-lat]].
- [7] S. Aoki *et al.* [HAL QCD Collaboration], Prog. Theor. Exp. Phys. **2012** (2012) 01A105 [arXiv:1206.5088 [hep-lat]].
- [8] N. Ishii *et al.* [HAL QCD Collaboration], Phys. Lett. **B712** (2012) 437 [arXiv:1203.3642 [hep-lat]].
- [9] Y. Ikeda *et al.* [HAL QCD Collaboration], Phys. Lett. **B729** (2014) [arXiv:1311.6214 [hep-lat]].
- [10] T. Inoue *et al.* [HAL QCD Collaboration], Phys. Rev. Lett. **106** (2011) 162002 [arXiv:1012.5928 [hep-lat]].
- [11] K. Murano *et al.* [HAL QCD Collaboration], Phys. Lett. **B735** (2014) 19 [arXiv:1305.2293 [hep-lat]].
- [12] T. Doi *et al.* [HAL QCD Collaboration], Prog. Theor. Phys. **127** (2012) 723.
- [13] T. Inoue *et al.* [HAL QCD Collaboration], Phys. Rev. Lett. **111** (2013) 112503 [arXiv:1307.0299 [hep-lat]].
- [14] K. Sasaki *et al.* Prog. Theor. Exp. Phys. (2015) 113B01 [arXiv:1504.01717 [hep-lat]].
- [15] PACS-CS Collaboration: S. Aoki, *et al.*, Phys. Rev. **D79** (2009) 034503.
- [16] K.U. Can, G. Erkol, B. Isildak, M. Oka and T.T. Takahashi, Phys. Lett. **B726** (2013).
- [17] M. Oka, K. Shimizu, and K. Yazaki, Nucl. Phys. **A464** (1987) 700.